Supplementary Information

Peroxidase-like bimetal Cu-Fe oxide mesoporous nano-spheres identified for efficient recognition of toxic *o*-Aminophenol and bioactive glutathione

Xuemei Zhou,[a,ξ] Lingmin Kong,[a,ξ] Junkai Hao,[a] Jing Feng,[a] Shuo Sun,[a] Chuanzhen Zhou,[b]

Yanmin Liu,[c] Zhengquan Yan,[a,*] Xiao Zhu,[a] Lei Hu[a,*]

[a]School of Chemistry and Chemical Engineering & Key Laboratory of Catalytic Conversion

and Clean Energy in Universities of Shandong Province, Qufu Normal University, Qufu, 273165,

China

[b]College of Chemical and Biological Engineering, Shandong University of Science and

Technology, Qingdao, 266590, China

[c]Qufu Agriculture-Technology Extension and Service Center, Qufu, 273100, China

Email: kaixinguolei333@163.com, yanzhq2008@163.com

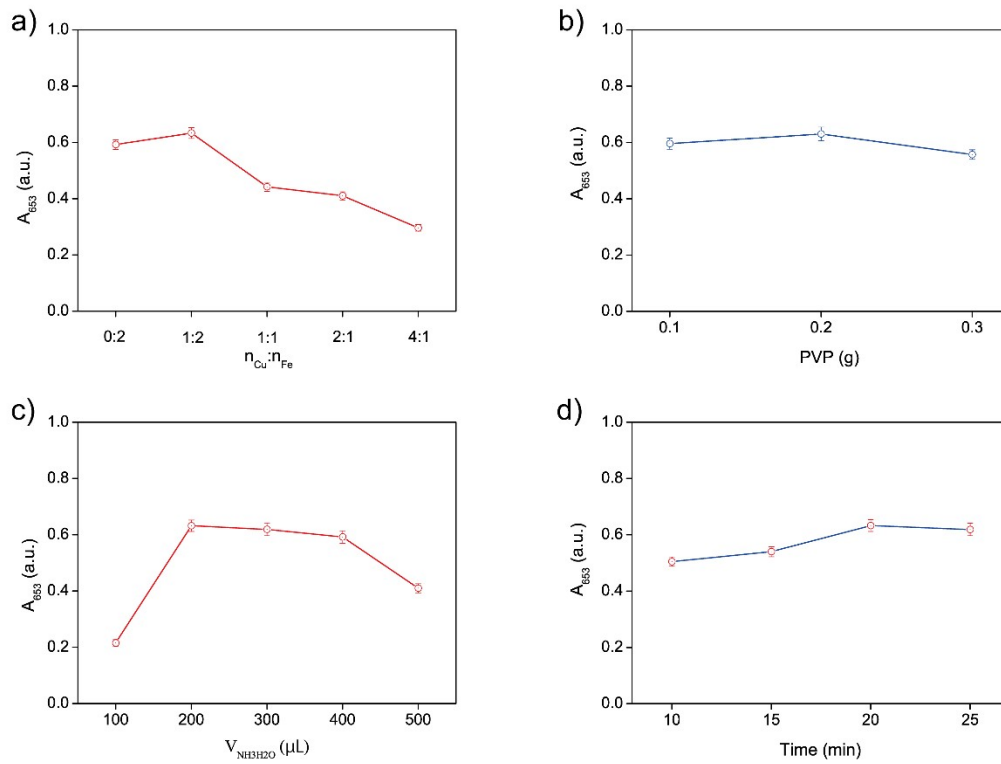[ξ] The two authors contributed equally to the work

Figure S1. The optimized conditions of a) mole feed ratios of Cu to Fe, b) PVP dosages, c) ammonia dosage and d) microwave radiation time.
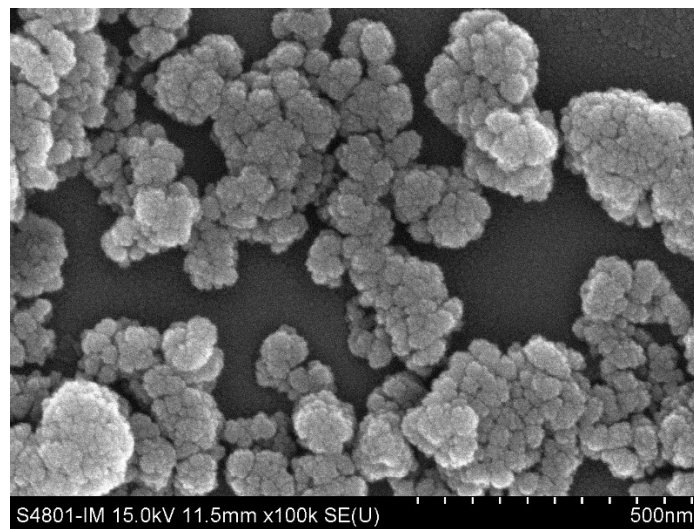

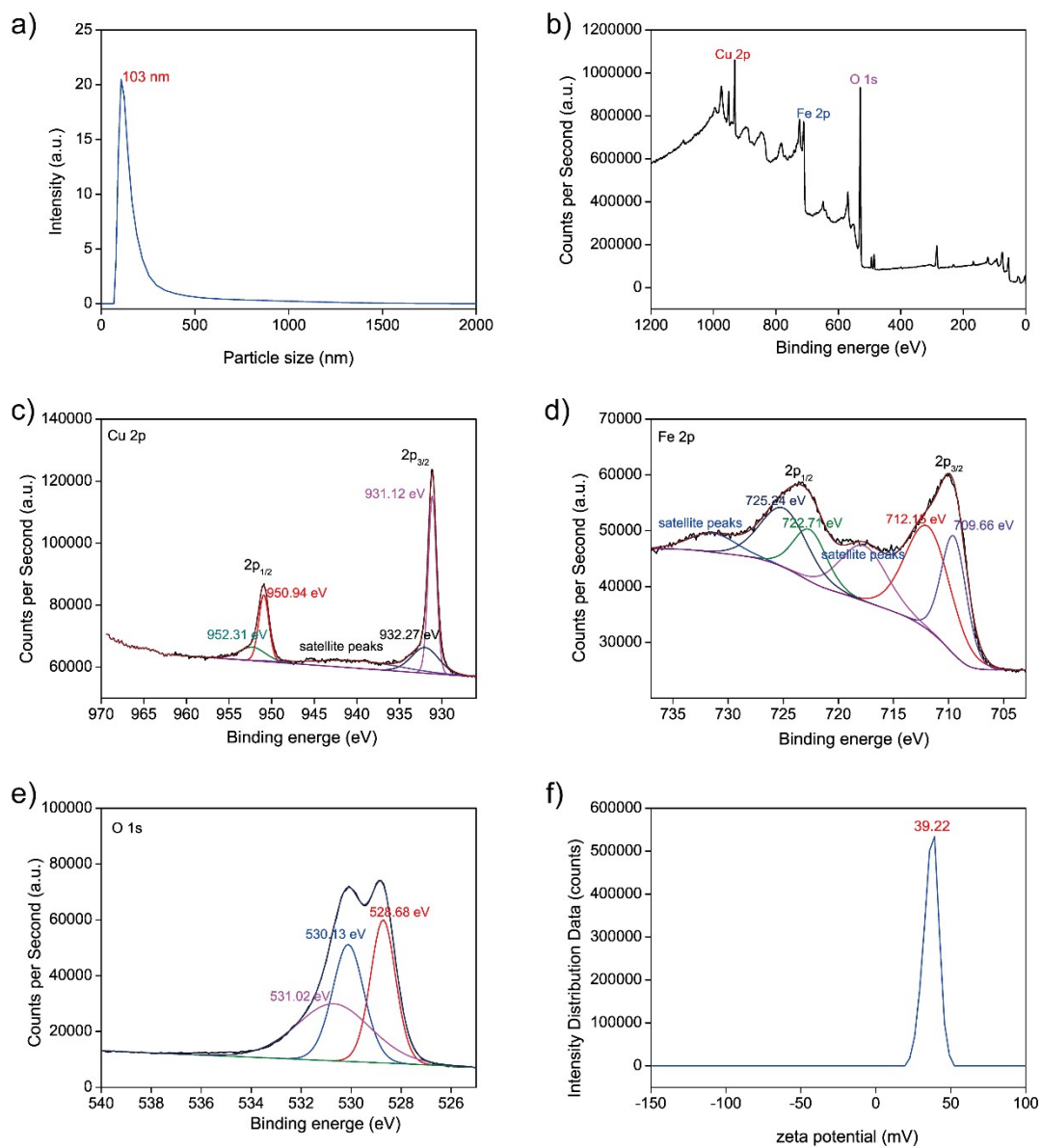**Figure S2**. SEM graph of the proposed Cu-Fe MNPs

Figure S3. a) DLS curve, b) XPS wide angle spectra, high-resolution spectra of c) Cu2p, d) Fe2p,
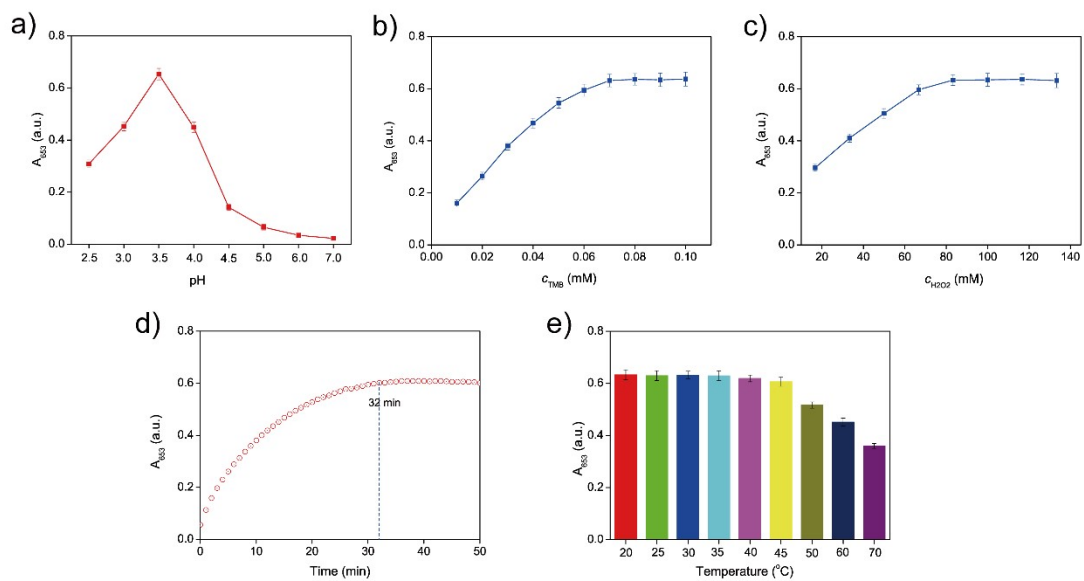
e) O1s and f) ζ potential of the proposed Cu-Fe MNPs

Figure S4. The effects of a) pH, b) TMB concentration, c) H_2O_2 concentration, d) reaction time and e) reaction temperature on absorbance intensity at 653 nm (A_{653}) of Cu-Fe MNPs
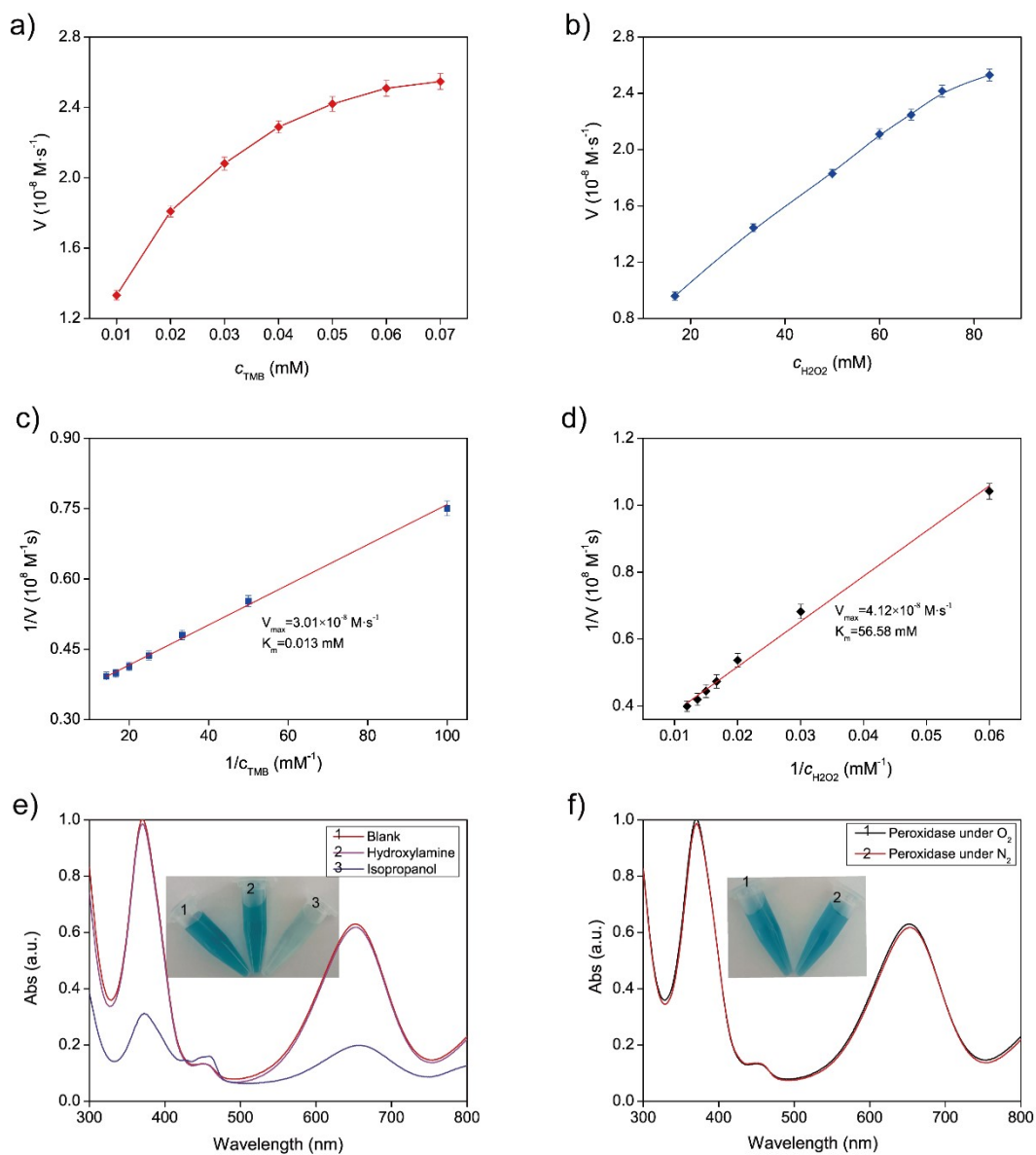
Figure S5. Steady-state kinetics of Cu-Fe MNPs with a) different c_{TMB}, b) c_{H2O2}; and the corresponding double-reciprocal plots of $1/v$ against c) $1/c_{TMB}$ and d) $1/c_{H2O2}$ with changing c_{TMB} or c_{H2O2} but fixed the others; UV-vis spectra and color changes (Insert) for Cu-Fe MNPs-TMB-H_2O_2 system e) in the presence of isopropanol and hydroxylammonium chloride and f) under air-saturated and N_2-saturated conditions

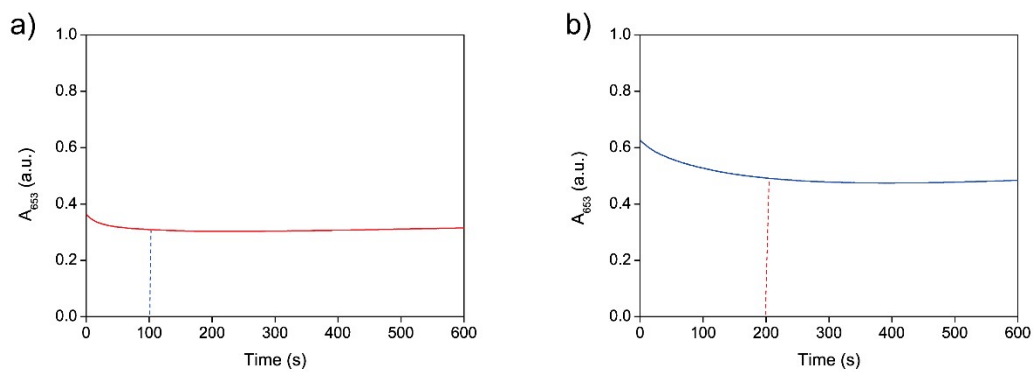**Figure S6**. Time response curves of A_{653} upon the addition of a) *o*-AP and b) GSH respectively
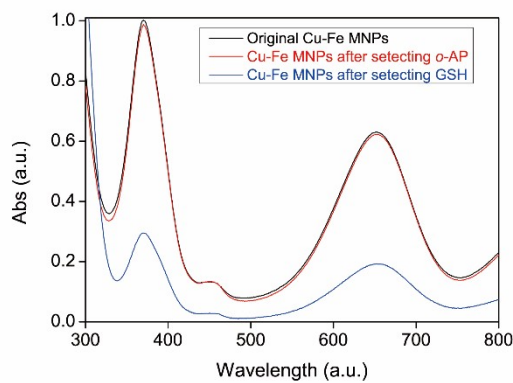

Figure S7. The comparison for UV-vis absorption spectra of TMB-H_2O_2 systems catalyzed by original Cu-Fe MNPs (Blank), Cu-Fe MNPs after detecting *o*-AP (Red) and Cu-Fe MNPs after detecting GSH (Blue) respectively (0.1 mg/mL Cu-Fe MNPs, pH 3.5, 0.07 mM TMB, 83.3 mM H_2O_2 and incubated 35 min at 25 °C)

Table S1. Calculation of initial reaction rate: The concentration of TMB-derived oxidation products was calculated by Lambert-Beer Law with a molar absorption coefficient of 39000 $M^{-1} \cdot cm^{-1}$

Time(s)	A	The concentration of TMB-derived oxidation products (M) ($c=A/\varepsilon b$, where $\varepsilon=39000\ M^{-1}\cdot cm^{-1}$, $b=1$ cm)	Rate $R=(c/t)_{average}$ ($M \cdot s^{-1}$)
30	0.111	2.85×10^{-6}	
60	0.125	3.21×10^{-6}	
90	0.139	3.56×10^{-6}	
120	0.152	3.87×10^{-6}	
150	0.164	4.21×10^{-6}	
180	0.176	4.51×10^{-6}	
210	0.188	4.82×10^{-6}	
240	0.199	5.11×10^{-6}	
270	0.209	5.36×10^{-6}	
300	0.219	5.62×10^{-6}	2.57×10^{-8}
330	0.231	5.89×10^{-6}	
360	0.24	6.15×10^{-6}	
390	0.252	6.41×10^{-6}	
420	0.261	6.67×10^{-6}	
450	0.269	6.89×10^{-6}	
480	0.278	7.15×10^{-6}	
510	0.289	7.38×10^{-6}	
540	0.297	7.62×10^{-6}	
570	0.305	7.82×10^{-6}	
600	0.314	8.05×10^{-6}	

Table S2. Comparing the steady-state kinetic parameters of the present Cu-Fe MNPs

with other nanomaterials-based peroxidase mimics reported previously

Nanomaterials	Substrates	K_m (mM)	V_{max} (10^{-8} M·s^{-1})	Refs.
Fe$_3$O$_4$ MNPs[1]	TMB	0.098	3.44	[1]
	H$_2$O$_2$	154	9.78	
HRP	TMB	0.434	10.00	[1]
	H$_2$O$_2$	3.7	8.71	
IrO$_2$/rGO[2]	TMB	0.276	42.77	[2]
	H$_2$O$_2$	229.4	372.9	
MA-Hem/Au-Ag[3]	TMB	2.39	1.42	[3]
	H$_2$O$_2$	2.71	11.4	
Cu NCs	TMB	0.648	5.96	[4]
	H$_2$O$_2$	29.16	4.22	
Cu-Fe MNPs	**TMB**	**0.013**	**3.01**	**This work**
	H$_2$O$_2$	**56.58**	**4.12**	

1. Fe$_3$O$_4$ MNPs: Fe$_3$O$_4$ magnetic nanoparticles
2. IrO$_2$/rGO: IrO$_2$ nano-particles on reduced graphene oxide (rGO) nanosheets
3. MA-Hem/Au-Ag: gold-silver bimetals into Hemin(Hem)-coupled melamine (MA) polymer matrix

Table S3. Comparing the determination of *o*-AP by Cu-Fe MNPs with other

nanomaterials reported previously

Materials	Method	Analytes	Linear range (µM)	LOD (µM)	Refs.
GNP-modified ITO microelectrodes[1]	dual-channel microchip electrophoresis	*o*-AP	1-500	0.41	[5]
	gas chromatography	*o*-AP		23.48	[6]
cationic p-(quaternary ammonium) calix[4]-arene	capillary electrophoresis	*o*-AP		2.64	[7]
SPCE[2]	Electrochemical	*o*-AP	0.2-100	0.07	[8]
NH$_2$-SBA-15/CPE[3]	Electrochemical	*o*-AP	0.3-18	0.05	[9]
Ce-CDs[4]	Fluorescent	*o*-AP	0.1-10	0.033	[10]
modified PDMS microchip[5]	microchips	*o*-AP	50-400	10.0	[11]
Triethylamine (pH 8)	Liquid chromatography	*o*-AP	9.17-450	4.22	[12]
Cu-Fe MNPs	**Colorimetry**	***o*-AP**	**0.33-12.67**	**0.016**	**This work**

1、GNP-modified ITO microelectrodes: A gold nanoparticle-modified indium tin oxide microelectrode

2、SPCE: Electrochemically pretreated screen-printed carbon electrodes.

3、NH$_2$-SBA15/CPE: Amino-functionalized SBA15 modified carbon paste electrode

4、Ce-CDs: Ceriumdoped carbon dots

5、modified PDMS microchip: Modified poly (dimethylsiloxane) (PDMS)microchips

Table S4. Comparing the determination of GSH by Cu-Fe MNPs with other

nanomaterials reported previously

Materials	Method	Analytes	Linear range (μM)	LOD (μM)	Refs.
MCE-CL [1]	microchip electrophoresis	GSH	3-600	0.96	[13]
Cy-AuNCs[2]	colorimetric	GSH	0-400	10.00	[14]
Met-AuNCs@MnO$_2$[3]	Fluorescent	GSH	1-700	0.068	[15]
AgNPs	colorimetric	GSH	0-400	4.11	[16]
TCFCl-GSH[4]	Fluorescent	GSH	0-500	0.45	[17]
Cu-Fe MNPs	**Colorimetry**	**GSH**	**0.66-21.67**	**0.033**	**This work**

1、 MCE-CL: microchip electrophoresis chemiluminescence
2、 Cy-AuNCs: Cytidine-Au nanoclusters
3、 Met-AuNCs@MnO$_2$: methionine-capped AuNCs and MnO$_2$
4、TCFCl-GSH: Long-wavelength TCF-based fluorescence probes

References：

1.　　L. Z. Gao, J. Zhuang, L. Nie, J. B. Zhang, Y. Zhang, N. Gu, T. H. Wang, J. Feng, D. L. Yang, S. Perrett and X. Yan, *Nat. Nanotechnol.*, 2007, **2**, 577-583.

2.　　X. L. Liu, X. H. Wang, Q. S. Han, C. Qi, C. Wang and R. Yang, *Talanta*, 2019, **203**, 227-234.

3.　　H. Liu, Y. Hua, Y. Y. Cai, L. P. Feng, S. Li and H. Wang, *Anal. Chim. Acta*, 2019, **1092**, 57-65.

4.　　L. Hu, Y. Yuan, L. Zhang, J. Zhao, S. Majeed and G. Xu, *Anal. Chim. Acta*, 2013, **762**, 83-86.

5.　　G. Z. Zhu, Q. H. Song, W. F. Liu, X. X. Yan, J. Xiao and C. P. Chen, *Anal. Methods*, 2017, **9**, 4319-4326.

6.　　A. Kumar and A. Panwar, *Microchim. Acta*, 1993, **111**, 177-182.

7.　　W. C. Yang, X. D. Yu, A. M. Yu and H. Y. Chen, *J. chromatography. A*, 2001, **910**, 311-318.

8.　　W. Y. Su, S. M. Wang and S. H. Cheng, *J. Electroanal. Chem.*, 2011, **651**, 166-172.

9.　　S. Duan, X. Zhang, S. Xu and C. L. Zhou, *Electrochim. Acta*, 2013, **88**, 885-891.

10.　　D. D. Zhao, Y. J. Huang, B. F. Shi, S. P. Li and S. L. Zhao, *ACS Sustain. Chem. Eng.*, 2021, **9**, 8136-8141.

11.　　Y. Xiao, K. Wang, X.-D. Yu, J.-J. Xu and H.-Y. Chen, *Talanta*, 2007, **72**, 1316-1321.

12.　　S. P. Wang and T. H. Huang, *Anal. Chim. Acta*, 2005, **534**, 207-214.

13.　　M. Shi, Y. Huang, J. J. Zhao, S. T. Li, R. J. Liu and S. L. Zhao, *Talanta*, 2018, **179**, 466-471.

14.   C. F. Jiang, C. Zhang, J. Song, X. J. Ji and W. Wang, *Spectrochim. Acta, Part A*, 2021, **250**, 119316.

15.   F. M. Sang, M. L. Li, S. Y. Yin, H. H. Shi, Y. Zhao and Z. Z. Zhang, *Spectrochim. Acta, Part A*, 2021, **256**, 119743.

16.   I. Sanskriti and K. K. Upadhyay, *New J. Chem.*, 2017, **41**, 4316-4321.

17.   A. C. Sedgwick, J. E. Gardiner, G. Kim, M. Yevglevskis, M. D. Lloyd, A. T. A. Jenkins, S. D. Bull, J. Yoon and T. D. James, *Chem. Commun.*, 2018, **54**, 4786-4789.